united nations
educational, scientific
and cultural
organization

international atomic
energy agency

the
abdus salam
international centre for theoretical physics

SMR 1232 - 35

XII WORKSHOP ON
STRONGLY CORRELATED ELECTRON SYSTEMS

17 - 28 July 2000

GIANT ENHANCEMENT OF THE THERMAL HALL CONDUCTIVITY K_{xy} IN THE SUPERCONDUCTOR $YBa_2Cu_3O_7$

N.P. ONG
Princeton University - Dept. of Physics
NJ-08544 Princeton, USA

Giant enhancement of the thermal Hall conductivity κ_{xy} in the superconductor $YBa_2Cu_3O_7$.

Y. Zhang[1], N. P. Ong[1], P. W. Anderson[1], D. A. Bonn[2], R. Liang[2] and W. N. Hardy[2]

[1] *Joseph Henry Laboratories of Physics, Princeton University, Princeton, New Jersey 08544*

[2] *Department of Physics, University of British Columbia, Vancouver, Canada.*

(February 18, 2000)

Abstract

In crystals of the superconductor $YBa_2Cu_3O_7$ of very high purity, the long quasiparticle (qp) lifetime τ leads to an enhanced (weak-field) thermal Hall conductivity κ_{xy} that undergoes a thousand-fold increase below the transition temperature T_c. At low temperatures, we confirm Simon-Lee scaling behavior for κ_{xy} and some of its striking consequences. The experiment impacts current debates on two aspects of qp behavior in cuprates: Does Landau quantization occur at the gap nodes, and does τ change abruptly at T_c?

In a superconductor, the electrons form a condensate that is a coherent superposition of Cooper pairs. Because of the 'rigidity' of the gap wave function, the condensate itself does not respond to most experimental probes. Instead, its properties are known from experiments that excite and measure its low-energy excitations, or quasiparticles. In the cuprate superconductors, d-wave symmetry of the gap function leads to a gap amplitude that vanishes at nodes on the Fermi Surface FS. Near each node, the contours of the qp energy form an anisotropic Dirac cone [1]. The interaction of the qp states with vortices is (thus far) an intractable problem that has received wide theoretical attention [2–6], but little experimental input. Microwave and terahertz experiments [7–9], and, more recently, angle-resolved photoemission spectroscopy (ARPES) [10,11], have produced a wealth of information on qp behavior in the cuprates in *zero* field. Recently, experiments investigating thermal transport properties, especially the thermal Hall effect [12–14], have also emerged as incisive probes of the quasiparticles, particularly in a strong magnetic field.

In a superconductor, an applied thermal gradient produces a heat current comprised of a quasiparticle and a phonon component (the condensate itself does not respond to the gradient). Krishana *et al.* [12] demonstrated that, when a magnetic field H is present, the qp heat current develops a transverse component that is observed as a thermal Hall conductivity κ_{xy} (by contrast, phonons cannot display a Hall effect since they are charge-neutral). Hence, κ_{xy} *selectively* senses the qp current alone.

Previous measurements of κ_{xy} were severely hampered by weak Hall signals, which limited reliable measurements to above 35 K [12,14]. A recent innovation is the growth of $YBa_2Cu_3O_y$ (YBCO) crystals in $BaZrCO_3$ (BZO) crucibles. Crystals grown in BZO crucibles show nearly perfect crystalline order (from x-ray rocking curves [15]) and very low impurity concentration. The concomitant increase in the (zero-field) qp lifetime τ results in strong enhancements of the qp charge and entropy currents. The most striking change, however, appears in the weak-field κ_{xy} which increases a thousand-fold between T_c and 30 K. These crystals enable κ_{xy} to be measured to $\sim$ 10 K, thus providing the first detailed picture of the low-T Hall response.

Among the cuprates, 90-K $YBa_2Cu_3O_7$ displays the largest in-plane thermal conductivity anomaly. In BZO-grown crystals, this anomaly is further enhanced, as shown in Fig. 1 (Panel C). The longitudinal thermal conductivity κ_{xx} ($-\nabla T \parallel \mathbf{a}$) in BZO crystals (solid circles) attains a peak value that is $\sim$ 80% larger than that seen in typical, non-BZO detwinned crystals (open circles). To isolate the qp current, we turn to κ_{xy}.

Figure 1 shows traces of κ_{xy} vs. H at high (Panel A) and low (B) temperatures [16]. As in earlier studies [12,14], the initial slope $\kappa_{xy}^0/B \equiv \lim_{B\to 0} \kappa_{xy}/B$ increases very rapidly as the temperature T falls below T_c. Further, the curves are strongly non-linear in H. Both features reflect a τ that increases rapidly with decreasing T. An important new feature, absent in previous studies, is the prominent 'overshoot' that produces a maximum in κ_{xy} at the field scale H_{max}. As T falls below 40 K (Panel B), the peak continues to narrow. For later reference, we note that, over a broad range of temperatures ($10 < T < 70$ K), H_{max} varies as T^2. Moreover, at low temperatures ($T < 28$ K), the peak magnitude κ_{xy}^{max} also scales as T^2.

The initial slope κ_{xy}^0/B, plotted as solid circles in Panel A of Fig. 2, undergoes a thousand-fold increase between T_c and 30 K (the T-linear variation of κ_{xy} above T_c are displayed as open circles [17]). We now show that this giant enhancement is driven by a 100-fold increase in the qp lifetime.

To extract the zero-field mean-free-path (mfp) from κ_{xy}^0/B, we apply the Boltzmann-equation approach [18], which should be valid in the *weak*-field regime $\omega_c\tau \ll 1$ (ω_c is the cyclotron frequency). In this semiclassical picture, a wavepacket constructed in state $\mathbf{k}$ carries an energy $E_\mathbf{k}$ with a group velocity $\mathbf{v_k} = \hbar^{-1}\nabla E_\mathbf{k}$ during its lifetime $\tau_\mathbf{k}$ (inset, Fig. 2(A)). Summing over the particle- and hole-like branches, we obtain the zero-H thermal conductivity $\kappa_e = c_e\langle v_\mathbf{k}\ell_\mathbf{k}\rangle/2$, where c_e is the 'qp heat capacity', and $\langle\cdots\rangle$ means averaging over a Dirac cone [19]. (Close to a node $\mathbf{k}_0$, we have $E_\mathbf{q} = \hbar\sqrt{(v_f q_1)^2 + (v_\Delta q_2)^2}$, where v_f and v_Δ are velocity parameters normal and parallel to the FS, and $\mathbf{q} = \mathbf{k} - \mathbf{k}_0$. We define the mfp $\ell \equiv v_f\tau_{\mathbf{k}_0}$.)

A *weak* field causes the wavepacket to move on a contour of $E_\mathbf{q}$, producing an energy

current transverse to $-\nabla T$ [inset, Fig. 2(A)]. The thermal Hall conductivity is then $\kappa_{xy} = \kappa_e \tan\theta$. We assume the thermal Hall angle $\tan\theta$ is proportional to $\omega_c\tau$, viz.

$$\tan\theta = \eta\omega_c\tau = \eta\ell/k_F\ell_B^2, \quad (B \to 0) \tag{1}$$

where k_f is the Fermi wavevector and $\ell_B = \sqrt{\hbar/eB}$ the magnetic length. The parameter η is less than 1 if ℓ is anisotropic around the FS. To determine $\tan\theta$, we first fit the profile of κ_{xx} vs. H to the empirical expression $\kappa_{xx}(B,T) = \kappa_e^0(T)/[1 + p|B|^\mu] + \kappa_{bg}(T)$, where the background term $\kappa_{bg}(T)$ is H-independent and identified with the phonon contribution. The initial Hall angle is then obtained as [14] $\tan\theta = \lim_{B\to 0} \kappa_{xy}(B)/[\kappa_{xx}(B) - \kappa_B]$. This procedure allows us to extract $\tan\theta$ (hence, ℓ using Eq. 1).

As a consistency check, we adopt a second way to obtain ℓ from κ_{xy}^0 that relies on measurements of the electronic heat capacity c_e. Using Eq. 1, we may write

$$\kappa_{xy}^0 = \frac{c_e v_f \ell^2 \eta}{4 k_f \ell_B^2}. \tag{2}$$

In a d-wave superconductor, $c_e = \alpha_c T^2$ for $T < T_c$. Using the measured value $\alpha_c \simeq 0.064$ mJK^{-3}mol^{-1} [20], we may invert Eq. 2 to find ℓ. We find that the values of ℓ obtained from the two methods share the *same* T dependence, but differ by a fixed factor of 1.5 if $\eta = 1$. By adjusting η to 0.6, we obtain numerical agreement between the two methods.

Figure 2(B) shows the T dependence of ℓ derived from the two methods. The agreement between the two sets of data is evidence that our assumption Eq. 1 is physically reasonable. Remarkably, between T_c and 20 K, the mfp increases by a factor of $\sim$120 from 80 A to 1 micron. In the expanded scale, we show that this increase is abrupt, starting slightly below T_c. [For comparison, $\tan\theta$ measured previously in a non-BZO crystal [14] is shown as $\times$. Based on the higher sensitivity in the present experiment, we now conclude that $\tan\theta$ does not lie on the extrapolated curve for the electrical Hall angle $\tan\theta_e$.]

Beyond the weak-field regime, we need a microscopic description of the qp thermal Hall current to properly understand κ_{xy} vs. H. However, because the theoretical situation is unsettled, we will adopt the scaling arguments of Simon and Lee [21]. This approach reveals some rather striking features in the data.

Close to the node, the linear energy dispersion $E = \hbar\bar{v}q$ ($\bar{v}$ is an average velocity) implies a general relation between k_BT and the magnetic length ℓ_B at a characteristic field scale B_s, viz.

$$k_BT = \hbar\bar{v}\sqrt{\frac{eB_s}{\hbar}}. \tag{3}$$

In addition to this general relation, Simon and Lee [21] have proposed that, at low T (<30 K for YBCO), the magnitude of κ_{xy} should scale as

$$\kappa_{xy}(H,T) \sim T^2 F_{xy}(\sqrt{H}/\alpha T), \tag{4}$$

where $\alpha \equiv k_B/\bar{v}\sqrt{e\hbar}$, and $F_{xy}(u)$ is a scaling function of the dimensionless parameter $u = \sqrt{H}/\alpha T$ (Simon and Lee write the argument of F_{xy} as $x = 1/u$). Hence, plots of κ_{xy}/T^2 versus $\sqrt{H}/T$ should collapse to the universal curve $F_{xy}(u)$.

We proceed to plot our results in this way in Fig. 3. While the curves above 28 K are spread out, the ones below collapse onto a common curve for $H < H_{max}$. Hence, below 28 K, the data rapidly converge to the scaling form in Eq. 4. Collectively, they determine experimentally the form of $F_{xy}(u)$. Its most notable feature is the nominally straight segment that extends from $u \simeq 0$ to just below $u_0 \equiv \sqrt{H_{max}}/\alpha T$, i.e. $F_{xy}(u) \sim u$ for $0 < u < u_0$. This simple form for F_{xy} implies that, below 25 K and for $H < H_{max}$, κ_{xy} reduces to the form

$$\kappa_{xy}(H,T) = C_0 T\sqrt{H}, \tag{5}$$

where the constant $C_0 = 1.51 \times 10^{-2}$ in SI units. Remarkably, when Eq. 5 applies, the magnitude of κ_{xy} is just proportional to $T\sqrt{H}$, and is insensitive to all transport quantities such as ℓ and θ. This interesting result has not been anticipated theoretically.

At larger values of u, F_{xy} attains a maximum value F_{xy}^0 before falling slowly. The T^2 dependence of the peak value κ_{xy}^{max} noted earlier in Fig. 1, is now seen to be a simple consequence of scaling behavior (i.e. $\kappa_{xy}^{max} \sim T^2 F_{xy}^0$).

Above 28 K, scaling no longer holds. Three field regimes are now apparent. In weak fields ($0 < H < H_x$), κ_{xy} is strictly linear in H. Above H_x, we enter a regime reminiscent

of the $\sqrt{H}$ behavior at low-T (the H-linear regime is too small to resolve below 28 K). This intermediate regime appears as straight-line segments in Fig. 3. Finally, closer to H_{max}, κ_{xy} deviates from $\sqrt{H}$ behavior, and goes through a broad maximum. Surprisingly, as noted earlier, the weaker scaling relation in Eq. 3 continues to hold: Between 15 and 70 K, the maximum in κ_{xy} occurs at the *same* x-coordinate in Fig. 3, i.e. $\sqrt{H_{max}} = 0.042\ T$. Substituting H_{max} for B_s in Eq. 3, we find that $\bar{v} \sim 8.0 \times 10^6$ cm/s, which is close to the geometric-mean velocity $\sqrt{v_f v_\Delta} \sim 6.8 \times 10^6$ cm/s (with $v_f = 1.78 \times 10^7$cm/s [10] and $v_f/v_\Delta \sim 7$).

In the semiclassical approximation, an excitation on the particle branch of the Dirac cone travels from points 1 to 2 in a time $\Delta t = (\hbar/eH) \int_1^2 ds_{\mathbf{k}} \mid \mathbf{v_k} \mid^{-1}$, where $s_{\mathbf{k}}$ is the arc length (inset Fig. 2). Identifying Δt with τ, we solve for the field H_{arc} (the field at which the qp just completes the path before it decays)

$$H_{arc} = \frac{\pi E}{e v_\Delta v_f \tau}. \tag{6}$$

Using the measured $\ell \simeq v_f \tau$ at each T and setting $E = k_B T$, we indicate H_{arc} as arrows in Fig. 3. This rough estimate shows that the peak is related to the maximum arc length of the dominant energy contour on the Dirac cone. Hence, the Hall curves provide direct information on *qp* behavior that are closely relevant to the current debate on how vortices affect the qp spectrum. Gorkov and Schrieffer [4] propose that, at 2, the excitation continues into the hole branch. They find that the states are quantized into Landau levels. One of us has proposed that Andreev reflection in fact occurs at the turning point 2, but Landau quantization still occurs [5]. However, a detailed numerical calculation by Franz and Tesanovic has not found evidence for Landau quantization [6]. Comparison of the present results with microscopic calculations will stringently narrow the possibilities, and may well be sufficient to settle the debate.

The new results on κ_{xy} also sharpen the issues in a different debate regarding qp lifetimes. Previously, evidence from terahertz [8] and heat transport [22,12] experiments showed that the qp lifetime undergoes a steep increase just below T_c. However, recent ARPES measure-

ments in $Bi_2Sr_2CaCu_2O_8$ (BSCCO) [10] show that the width $\Delta\omega$ of the qp spectral function smoothly continues its $1/T$ dependence through T_c ($\Delta\omega \simeq 1/(k_f\ell)$). The present experiment shows in effect that, with a step-wise improvement in sample purity, the rate of increase in ℓ changes even more abruptly below T_c [Fig. 2(B)]. This exacerbates the disagreement with ARPES. [In BSCCO, ℓ is considerably shorter. Nonetheless, κ_{xy} also shows an abrupt change in slope at T_c [23].] The clear discrepancy between the transport and ARPES results suggests that the nature of the excitations in cuprates is poorly understood. From the transport viewpoint, the carrier lifetimes are short above T_c because of intense scattering of the carriers (likely from electron-electron processes). When long-range phase coherence sets in at T_c, the intense scattering decreases precipitously, leading to a steep increase in excitation lifetimes (which is not observed in low-T_c superconductors). The rapid increase in ℓ below T_c apparently does not translate into a discernible narrowing of the qp width in ARPES. Understanding this discrepancy presents a strong challenge to theory.

REFERENCES

[1] For a review, see P. A. Lee, Science **277**, 5322 (1997).

[2] C. Kubert, P. J. Hirschfeld, Phys. Rev. Lett. **80**, 4693 (1998).

[3] M. Franz, Phys. Rev. Lett. **82**, 1760 (1999).

[4] L. P. Gorkov, J. R. Schrieffer, Phys. Rev. Lett. **80**, 3360 (1998).

[5] P. W. Anderson, cond-mat/9812063.

[6] M. Franz, Z. Tesanovic, cond-mat/9903152.

[7] D. A. Bonn *et al.*, Phys. Rev. Lett. **68**, 2390 (1992); A. Hosseini et al., Phys. Rev. B **60**, 1349 (1999).

[8] Martin C. Nuss *et al.*, Phys. Rev. Lett. **66**, 3305 (1991).

[9] J. Corson, R. Mallozzi, J. Orenstein, J.N. Eckstein,, I. Bozovic, Nature **398**, 221 (1999).

[10] T. Valla *et al.*, Science **285**, 2110 (1999).

[11] A. Kaminski *et al.*, Phys. Rev. Lett. **84**, xxx (2000), Feb. 21st, 2000.

[12] K. Krishana, J. M. Harris,, N. P. Ong, Phys. Rev. Lett. **75**, 3529 (1995).

[13] B. Zeini *et al.*, Phys. Rev. Lett. **82**, 2175 (1999).

[14] K. Krishana *et al.*, Phys. Rev. Lett. Phys. Rev. Lett. **82**, 5108 (1999).

[15] Ruixing Liang, D.A. Bonn, W.N. Hardy, Physica C **304**, 105 (1998).

[16] With the thermal gradient $-\nabla T \parallel \mathbf{a} \parallel \mathbf{x}$ and the field $\mathbf{H} \parallel \mathbf{c} \parallel \mathbf{z}$, the thermal Hall current is $\parallel \mathbf{y}$. Above 35 K, the 'Hall' gradient $-\partial_y T$ is measured continuously with a chromel-constantan thermocouple as H is swept slowly (0.2 T/min.). Below 35 K (Fig. 1(B)), we adopt a high-resolution mode. Each point is taken with H stabilized. The signal is sampled with $-\partial_x T$ turned on, then off. Each Hall trace is the average of two

traces, from -14 to 14 T and from 14 to -14 T (below 5 T, the hysteresis between the two traces is of the order of the fluctuations in the signal.)

[17] Y. Zhang *et al.*, Phys. Rev. Lett. **84**, xxx (2000), *in press.*

[18] J. Bardeen, Rickayzen, Tewordt, Phys. Rev. **113**, 982 (1959).

[19] In the Boltzmann equation approach the thermal conductivity is $\kappa_e = T^{-1}\sum_{\mathbf{k}}(-\partial f/\partial E_{\mathbf{k}})E_{\mathbf{k}}^2 v_{\mathbf{k},x}^2 \tau_{\mathbf{k}}$. The qp heat capacity c_e has the same kernel, but without the factor $v_{\mathbf{k},x}^2\tau_{\mathbf{k}}$.

[20] D. A. Wright *et al.*, Phys. Rev. Lett. **82**, 1550 (1999).

[21] Steve H. Simon, Patrick A. Lee, Phys. Rev. Lett. **78**, 1548 (1997).

[22] R.C. Yu, M. B. Salamon, J. P. Lu, W. C. Lee, Phys. Rev. Lett. **69**, 1431 (1992).

[23] Y. Zhang, Y. Wang, N.P. Ong, *to be published.*

[24] The research is supported by the U.S. National Science Foundation (Grant NSF-DMR 9809483, at Princeton), and the Natural Science and Engineering Research Council (Canadian NSERC) and the Canadian Institute for Advanced research (CIAR) at U. British Columbia. N.P.O. also acknowledges support from the U.S. Office of Naval Research (Contract N00014-98-10081) and the New Energy and Industrial Tech. Develop. Org., Japan (NEDO). We thank T.V. Ramakrishnan for valuable comments.

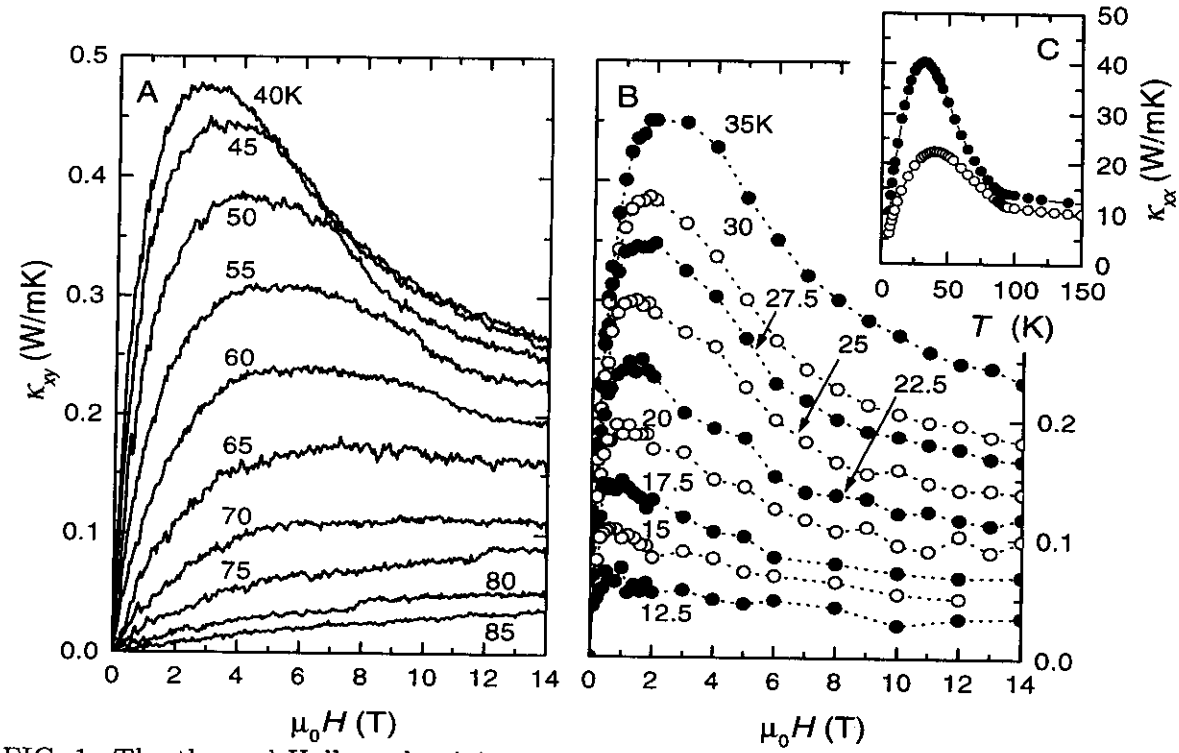

FIG. 1. The thermal Hall conductivity κ_{xy} vs. H in BZO-grown $YBa_2Cu_3O_{6.99}$ ($T_c = 89$ K) at high temperatures (85 to 40 K in Panel A), and low temperatures (35 to 12.5 K in Panel B). As T decreases below T_c, the initial slope κ^0_{xy}/B increases sharply. The prominent peak in κ_{xy} below 55 K is a new feature in BZO-grown YBCO. Panel C compares the zero-field $\kappa_{xx} \equiv \kappa_a$ in the BZO-grown crystal (solid circles) with a detwinned non-BZO grown crystal (open).

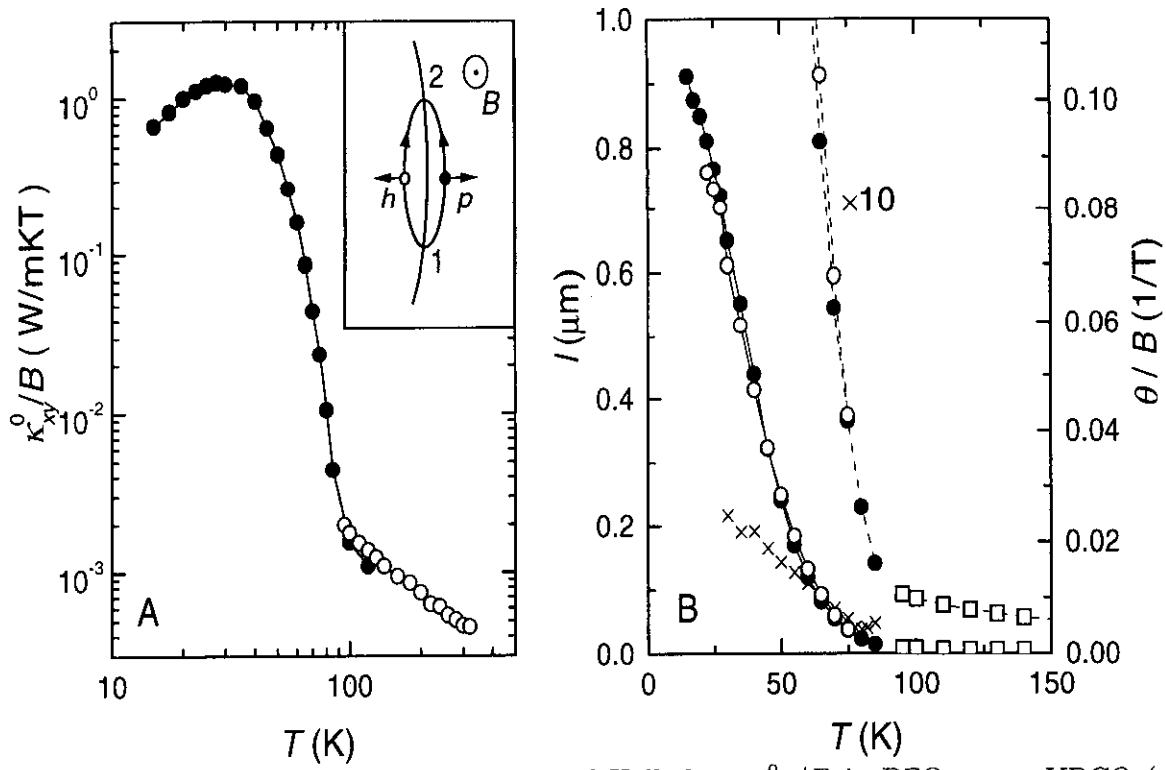

FIG. 2. (A) The T dependence of the initial Hall slope κ_{xy}^0/B in BZO-grown YBCO (solid circles). Between T_c and 30 K, κ_{xy}^0/B increases by 10^3. The $1/T$ dependence of κ_{xy}^0/B above T_c (measured in a non-BZO grown YCBO) is shown as open circles. The inset shows a qp energy contour on the Dirac cone. Group velocities on the particle- (p) and hole-like (h) branches are indicated. Panel B displays the zero-field mean-free-path ℓ extracted from the weak-field Hall angle $\tan\theta$ (open circles), and from Eq. 2 (closed). The *equivalent* values of θ/B are shown on the right scale. The symbols ($\times$) represent $\tan\theta$ measured in a non-BZO detwinned YBCO crystal (Krishana *et al.* [14]). The expanded scale (dashed lines) highlights the steep increase below T_c. To extract ℓ, we used the values $\eta = 0.60$, $v_f = 1.78 \times 10^7$ cm/s, and $k_f = 0.8A^{-1}$.

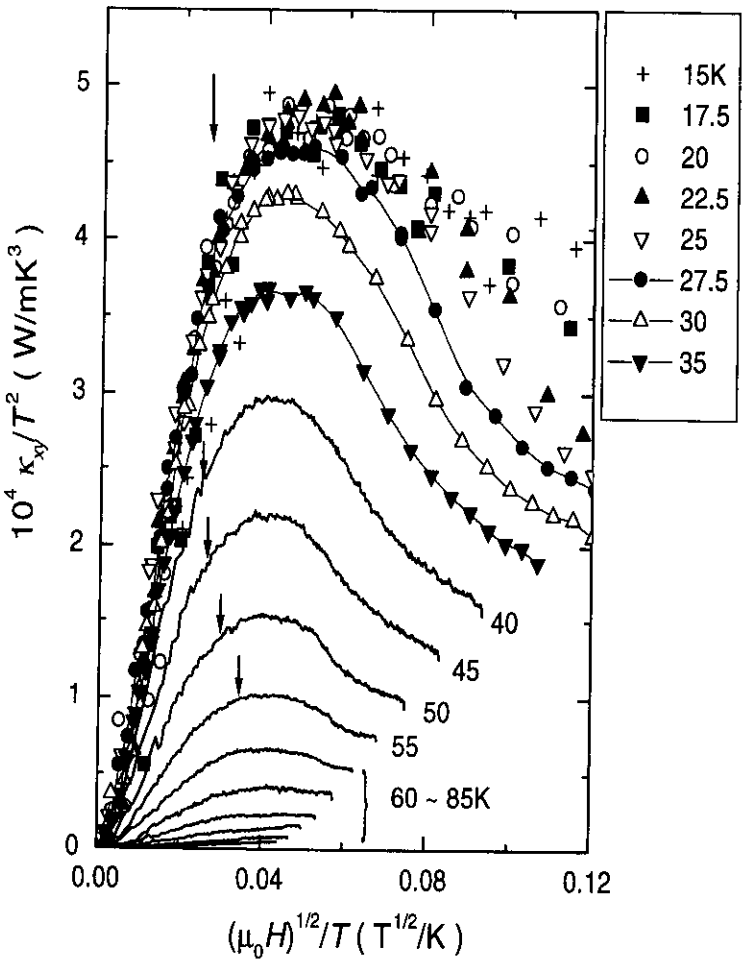

FIG. 3. Simon-Lee scaling plot of κ_{xy}/T^2 versus $\sqrt{H}/T$ (Eq. 4). Below 28 K, the curves collapse onto a 'universal' curve $F_{xy}(u)$. Above 28 K, scaling is violated. However, the peaks still occur at the same x-coordinate ($\sqrt{H_{max}}/T = 0.042$). The arrows indicate the field scale H_{arc} defined in Eq. 6.